XLI CILAMCE
XLI Ibero-Latin American Congress on Computational Methods in Engineering
16-19 November, 2020 FOZ DO IGUAÇU PARANÁ - BRAZIL

Comparison of the natural frequencies of a reference wind turbine blade using the finite element method with Euler-Bernoulli and Timoshenko beam formulations

João Pedro Tavares Pereira dos Santos[1], Guilherme Ribeiro Begnini[1]

[1]*Federal University of Bahia, Polytechnic School, Department of Mechanical Engineering*
Rua Prof. Aristídes Novis, 2, Federação, 40210-630, Salvador, Bahia, Brazil
jptpsantos@gmail.com, guilherme.begnini@ufba.br

Abstract. The development of horizontal axis wind turbines brought longer blades and taller towers, which incurs in structures more susceptible to vibration problems. The vibrational behavior of the blades and the tower are studied separately at a first stage and each structure is typically modeled as a cantilever beam, with the aid of the finite element method. The most common beam models are the Euler-Bernoulli Beam Model and Timoshenko Beam Model, both used on this work. The key differences between those two models are that the shear stress and the rotatory inertia effects are ignored on the first one, which generate some discrepancies among the results. In the present work, a finite element method code is implemented for both beam formulations to determine the natural frequencies of a reference wind turbine blade, whose properties were obtained in the literature. The code was first validated by comparing the computed and theoretical results for a cantilever beam with rectangular cross section, and then applied to the wind turbine blade. For both structures analyzed it is shown that the natural frequencies obtained with Timoshenko model are lower than the ones obtained with Euler-Bernoulli model, and that the magnitude of difference increases with mode order.

Keywords: Modal Analysis, Finite Elements, Euler-Bernoulli, Timoshenko, Wind Turbine Blade.

1 Introduction

On the latest years, in searching for more efficiency, power generation capacity and viability of implementation, longer and more flexible blades, together with taller towers, were developed for horizontal axis wind turbines. These characteristics increase the importance of aeroelastic analysis of these structures, which allows to determine how the oscillatory behavior will be in the presence of air flow (Hansen [1]).

For aeroelastic analysis, two distinct mathematical models must be coupled: one to represent the structural dynamics and other to represent the aerodynamics of the wind turbine (Wang et al. [2]). The structural dynamics model aims to determine the natural frequencies and vibrational mode shapes and is the focus of this paper.

At a first modelling stage, the blade and tower are analyzed separately and then assembled to represent the structural dynamics of the complete wind turbine, whose most common configuration is composed of one tower and three blades. The blade and tower structures are traditionally modeled as cantilever beams (clamped-free boundary condition) and the finite element method is used to account for the variation of properties along their length. Beam properties are obtained from more detailed finite element models, which uses solid and shell elements, and are developed with tension analysis in focus.

Among the beam elements formulations, the Euler-Bernoulli Beam, or Classical Beam Theory, is the most used one, given it ease of implementation and large reference material availability. However, it neglects the effects of shear stresses and rotatory inertia, which can incur in some errors. These effects are included in the Timoshenko beam element, making it a better representation of reality.

In the present work, a finite element method code is implemented for both beam formulations, Euler-Bernoulli and Timoshenko, in order to determine the natural frequencies of the DTU 10MW reference wind turbine

(RWT) blade, whose properties were obtained in Bak et al.[3]. The code was first validated by comparing the computed and theoretical results for a cantilever beam with rectangular cross section, and then applied to the wind turbine blade. The paper presents the theoretical expressions used to compute the natural frequencies and the finite element mass and stiffness matrices for both beam models, followed by the results obtained for the two structures analyzed and a discussion of the differences between Euler-Bernoulli and Timoshenko results.

2 Theoretical Equations for Natural Frequencies

Theoretical equations for natural frequencies of uniform beams (constant cross section and material properties along their length) considering the Euler-Bernoulli theory (EB) and Timoshenko beam theory (TBT) are presented in this section. The equations for EB are found in different vibration textbooks (Blevins [4], Rao [5], Inman [6], Craig & Kurdila [7]), while the equations for TBT are more restricted, being Huang [8] the reference for this paper. These equations depend on the boundary conditions defined at the beam ends. As the focus of this paper is on the clamped-free boundary condition (cantilever beam), only this condition will be considered.

The equations for axial and torsional vibrations are given in eq. (1) and eq. (2), respectively, where ω is the natural frequency (in rad/s), n is the mode number, L is the beam length, E is the Young's Modulus, ρ is the specific mass, G is the shear modulus, J is the torsional constant and I_P the polar moment of inertia. These equations apply to both beam models since the shear stress and the rotatory inertia affect only the transverse vibration modes.

$$\omega_n^{Axial} = \frac{(2n-1)\pi}{2L}\sqrt{\frac{E}{\rho}} \tag{1}$$

$$\omega_n^{Torsional} = \frac{(2n-1)\pi}{2L}\sqrt{\frac{GJ}{\rho I_p}} \tag{2}$$

The equation for transverse vibration considering EB is given in eq. (3), where I is the area moment of inertia, A is the cross section area and $(\beta_n L)$ is the weighted frequency, which is given by Inman [6] for the clamped-free boundary condition.

$$\omega_n^{EB} = (\beta_n L)^2\sqrt{\frac{EI}{\rho A L^4}} \tag{3}$$

A similar equation for transverse vibration considering TBT is given in eq. (4), but for this case the factors b_n do not have fixed values, and need to be obtained solving the frequency equation given in eq. (5), which is valid for the clamped-free boundary condition.

$$\omega_n^{TBT} = b_n\sqrt{\frac{EI}{\rho A L^4}} \tag{4}$$

$$2 + [b^2(r^2 - s^2)^2 + 2]\cosh b\alpha \cos b\beta - \frac{b(r^2+s^2)}{(1 - b^2 r^2 s^2)^{1/2}}\sinh b\alpha \sin b\beta = 0 \tag{5}$$

The parameters r^2, s^2, α and β are defined in eqs. (6)-(9). The factor κ in eq. (7) is the shear coefficient, which depends on the cross-section geometry.

$$r^2 = \frac{I}{AL^2} \tag{6}$$

$$s^2 = \frac{EI}{\kappa AGL^2} \tag{7}$$

$$\alpha = \frac{1}{\sqrt{2}}\left\{-(r^2+s^2) + \left[(r^2-s^2)^2 + \frac{4}{b^2}\right]^{1/2}\right\}^{1/2} \tag{8}$$

$$\beta = \frac{1}{\sqrt{2}}\left\{+(r^2+s^2) + \left[(r^2-s^2)^2 + \frac{4}{b^2}\right]^{1/2}\right\}^{1/2} \tag{9}$$

Equation (5) is valid for the case of

$$\left[(r^2 - s^2) + \frac{4}{b^2}\right]^{1/2} > (r^2 + s^2) \tag{10}$$

If the condition of eq. (10) is not satisfied some modifications are necessary in eqs. (5), (8) and (9), as presented by Huang [8]. The solution of eq. (10) is obtained by plotting the equation for a range of b values and finding the values at which the curve crosses zero.

3 Finite Element Method Procedure

The natural frequencies and mode shapes of an undamped multiple degree of freedom system are obtained by solving the following eigenvalue problem

$$[[K] - \omega^2[M]]\{X\} = \{0\} \tag{11}$$

where $[K]$ is the stiffness matrix, $[M]$ the mass matrix, ω the natural frequency and $\{X\}$ the vector that contains the corresponding mode shape. Both matrices are square and have dimension equal to the numbers of degrees of freedom of the system. A non-trivial solution of eq.(11) is obtained for

$$\Delta = |[K] - \omega^2[M]| = 0 \tag{12}$$

whose solution gives the values of the squared natural frequencies (ω^2).

The finite element method is used as an effective tool to obtain the stiffness and mass matrices of structures with complex geometry (Cook et al. [9]; Craig & Kurdila [7]). The basic idea is to divide the complex geometry into small parts with a much simpler geometry, such as lines, triangular or trapezoidal plates and tetrahedron or hexahedron solids. These simple parts are named elements, and their connection to each other occur at the extremities, named nodes. Stiffness and mass matrices are available for different types of elements, and their assembly provides the matrices for the complete structure.

For the particular case of line elements, depending on the degrees of freedom and mathematical assumptions that are considered, different element stiffness (k_e) and mass (m_e) matrices are obtained. This work considers all possible vibration directions for a line element: axial, torsional and transverse (bending). The axial and torsional element matrices have dimension 2 x 2 and are represented as (Craig & Kurdila [7])

$$k_e^{Axial} = \frac{EA}{L}\begin{bmatrix} 1 & -1 \\ -1 & 1 \end{bmatrix} \tag{13}$$

$$m_e^{Axial} = \frac{\rho AL}{6}\begin{bmatrix} 2 & 1 \\ 1 & 2 \end{bmatrix} \tag{14}$$

$$k_e^{Torsional} = \frac{GJ}{L}\begin{bmatrix} 1 & -1 \\ -1 & 1 \end{bmatrix} \tag{15}$$

$$m_e^{Torsional} = \frac{\rho I_p L}{6}\begin{bmatrix} 2 & 1 \\ 1 & 2 \end{bmatrix} \tag{16}$$

It is important to point that the mass matrices used in this work are referred as “consistent mass” matrices, and they consider that the mass is uniformly distributed along the element. An alternative representation is the “lumped mass” matrices, which consider that the mass is concentrated at the nodes.

The matrices for transverse vibration have dimension 4 x 4 and are distinct for Euler-Bernoulli theory (EB) and for Timoshenko beam theory (TBT). For EB the element matrices are

$$k_e^{EB} = \begin{bmatrix} \frac{12EI}{L^3} & \frac{6EI}{L^2} & -\frac{12EI}{L^3} & \frac{6EI}{L^2} \\ \frac{6EI}{L^2} & \frac{4EI}{L} & -\frac{6EI}{L^2} & \frac{2EI}{L} \\ -\frac{12EI}{L^3} & -\frac{6EI}{L^2} & \frac{12EI}{L^3} & -\frac{6EI}{L^2} \\ \frac{6EI}{L^2} & \frac{2EI}{L} & -\frac{6EI}{L^2} & \frac{4EI}{L} \end{bmatrix} \tag{17}$$

$$m_e^{EB} = \frac{\rho AL}{420}\begin{bmatrix} 156 & 22L & 54 & -13L \\ 22L & 4L^2 & 13L & -3L^2 \\ 54 & 13L & 156 & -22L \\ -13L & -3L^2 & -22L & 4L^2 \end{bmatrix} \tag{18}$$

For TBT, a correction factor is included to account for the effects of shear stress

$$\Phi = \frac{12EI}{\kappa GAL^2} \tag{19}$$

and the TBT element stiffness matrix is written as (Przemieniecki [10])

$$k_e^{TBT} = \begin{bmatrix} 12\bar{b} & 6\bar{b}L & -12\bar{b} & 6\bar{b}L \\ 6\bar{b}L & (4+\Phi)\bar{b}L^2 & -6\bar{b}L & (2-\Phi)\bar{b}L^2 \\ -12\bar{b} & -6\bar{b}L & 12\bar{b} & -6\bar{b}L \\ 6\bar{b}L & (2-\Phi)\bar{b}L^2 & -6\bar{b}L & (4+\Phi)\bar{b}L^2 \end{bmatrix} \tag{20}$$

where

$$\bar{b} = \frac{EI}{(1+\Phi)L^3} \tag{21}$$

The TBT element mass matrix (m_e^{TBT}) is divided in two parts (Przemieniecki [10]). The first one includes the shear stress effects (m_{e1}^{TBT}) and the second one the rotatory inertia effects (m_{e2}^{TBT}), as defined in eqs. (22)-(24).

$$m_e^{TBT} = m_{e1}^{TBT} + m_{e2}^{TBT} \tag{22}$$

$$m_{e1}^{TBT} = \frac{\rho AL}{(1+\Phi)^2} \begin{bmatrix} m_1 & m_2 & m_3 & -m_4 \\ m_2 & m_5 & m_4 & -m_6 \\ m_3 & m_4 & m_1 & -m_2 \\ -m_4 & -m_6 & -m_2 & m_5 \end{bmatrix} \tag{23}$$

$$m_{e2}^{TBT} = \frac{\rho AL}{(1+\Phi)^2} \left(\frac{r}{L}\right)^2 \begin{bmatrix} m_7 & m_8 & -m_7 & m_8 \\ m_8 & m_9 & -m_8 & m_{10} \\ -m_7 & -m_8 & m_7 & -m_8 \\ m_8 & m_{10} & -m_8 & m_9 \end{bmatrix} \tag{24}$$

where

$$r = \sqrt{\frac{I}{A}} \tag{25}$$

$$m_1 = \frac{13}{35} + \frac{7}{10}\Phi + \frac{1}{3}\Phi^2 \tag{26}$$

$$m_2 = \left(\frac{11}{210} + \frac{11}{120}\Phi + \frac{1}{24}\Phi^2\right)L \tag{27}$$

$$m_3 = \frac{9}{70} + \frac{3}{10}\Phi + \frac{1}{6}\Phi^2 \tag{28}$$

$$m_4 = \left(\frac{13}{420} + \frac{3}{40}\Phi + \frac{1}{24}\Phi^2\right)L \tag{29}$$

$$m_5 = \left(\frac{1}{105} + \frac{1}{60}\Phi + \frac{1}{120}\Phi^2\right)L^2 \tag{30}$$

$$m_6 = \left(\frac{1}{140} + \frac{1}{60}\Phi + \frac{1}{120}\Phi^2\right)L^2 \tag{31}$$

$$m_7 = \frac{6}{5} \tag{32}$$

$$m_8 = \left(\frac{1}{10} - \frac{1}{2}\Phi\right)L \tag{33}$$

$$m_9 = \left(\frac{2}{15} + \frac{1}{6}\Phi + \frac{1}{3}\Phi^2\right)L^2 \tag{34}$$

$$m_{10} = \left(-\frac{1}{30} - \frac{1}{6}\Phi + \frac{1}{6}\Phi^2\right)L^2 \tag{35}$$

Noting that the transverse vibration can occur in two directions (referred in this work as flapwise and edgewise directions), it is possible to assemble three-dimensional beam element matrices, of dimension 12 x 12, that account for all possible vibration directions. However, the separate matrices were used in this work in order to facilitate the description of mode shapes. The use of the 12 x 12 matrices would require the plotting and inspection of the mode shapes to allow their description.

4 Validation Case: uniform beam with rectangular cross section

The validation case selected for this paper is a uniform cantilever beam with rectangular cross section, made of structural steel (E=200 GPa, G=76.9 GPa and ρ=7850 kg/m^3). The beam is 1 m long and the cross section has 0.2 m x 0.1 m, being a the longer and b the shorter sides. The coordinate system is chosen such as the x direction is aligned with the beam length, the y direction is aligned with the longer side and the z direction is aligned with the shorter side. Vibrations in the z direction are named vertical transverse vibrations (or flapwise vibrations) and vibrations in the y direction are named lateral transverse vibrations (or edgewise vibrations).

Some of the parameters needed for the theoretical equations presented in Section 2 are dependent on the cross section. These parameters are presented in eqs. (36)-(40) for the rectangular cross section. Eq. (36) is approximate and was taken from Young & Budynas [11]. In eq. (40) υ is the Poisson coefficient.

$$J = (\frac{a}{2})(\frac{b}{2})^3 \left(\frac{16}{3} - 3.36 \frac{(\frac{b}{2})}{(\frac{a}{2})} \left(1 - \frac{(\frac{b}{2})^4}{12(\frac{a}{2})^4} \right) \right) \tag{36}$$

$$I_y = \frac{ab^3}{12} \tag{37}$$

$$I_z = \frac{ba^3}{12} \tag{38}$$

$$I_p = I_y + I_z \tag{39}$$

$$\kappa = \frac{10(1+\upsilon)}{12+11\upsilon} \tag{40}$$

The theoretical and FEM results for EB and TBT are presented in Table 1 For each beam formulation the differences between the computational and theoretical results are assessed using eq. (41).

$$\delta = \frac{FEM\ Result - Theoretical\ Result}{Theoretical\ Result} \tag{41}$$

The analysis was limited to 16 modes, which are ordered in ascending frequency values for EB. An excellent agreement between computational and theoretical results is obtained for both beam formulations, with a maximum difference of 0.2%, thus validating the FEM implementation for EB and TBT. The FEM implementation considered 100 elements.

A comparison of FEM results between TBT and EB is also presented in Table 1, in the last column. The difference is computed using eq. (42). The same values are obtained for axial and torsional modes, as expected. For the transverse vibration modes, it is shown that the TBT frequencies are lower than the EB frequencies, and that the magnitude of the difference increases with mode order. This behavior is illustrated for the vertical (flapwise) and lateral (edgewise) transverse modes in Figure 1 (a). A difference of about 40% is obtained for the 4th flapwise mode, which is considered a high value, indicating that the use of TBT can significantly improve the computation of natural frequencies depending on the beam dimensions and number of modes required for a particular problem.

$$\delta = \frac{TBT\ Result - EB\ Result}{EB\ Result} \tag{42}$$

Table 1 – Natural frequency results for uniform beam.

Description	Theoretical Freq. EB (Hz)	FEM Freq. EB (Hz)	Difference EB, δ	Theoretical Freq. TBT (Hz)	FEM Freq. TBT (Hz)	Difference TBT, δ	Difference FEM EB and TBT
1st Flapwise	81.37	81.54	0.20%	80.76	80.91	0.19%	-0.77%
1st Edgewise	162.99	163.08	0.05%	158.10	158.22	0.08%	-2.98%
2nd Flapwise	509.97	510.99	0.20%	484.33	485.20	0.18%	-5.05%
1st Torsion	580.38	580.03	-0.06%	580.38	580.03	-0.06%	0.00%
2nd Edgewise	1021.47	1022.00	0.05%	853.42	853.65	0.03%	-16.47%
1st Axial	1261.89	1261.90	0.00%	1261.89	1261.90	0.00%	0.00%
3rd Flapwise	1427.92	1430.80	0.20%	1275.07	1277.20	0.17%	-10.74%
2nd Torsion	1741.15	1740.20	-0.05%	1741.15	1740.20	-0.05%	0.00%
4th Flapwise	2798.16	2803.80	0.20%	2315.32	2318.80	0.15%	-17.30%
3rd Edgewise	2860.14	2861.60	0.05%	2034.21	2034.70	0.02%	-28.90%
3rd Torsion	2901.92	2900.80	-0.04%	2901.92	2900.80	-0.04%	0.00%
2nd Axial	3785.66	3786.00	0.01%	3785.66	3786.00	0.01%	0.00%
4th Torsion	4062.68	4062.20	-0.01%	4062.68	4062.20	-0.01%	0.00%
5th Flapwise	4625.56	4634.80	0.20%	3527.98	3533.00	0.14%	-23.77%
5th Torsion	5223.45	5224.50	0.02%	5223.45	5224.50	0.02%	0.00%
4th Edgewise	5604.74	5607.50	0.05%	3377.03	3382.20	0.15%	-39.68%

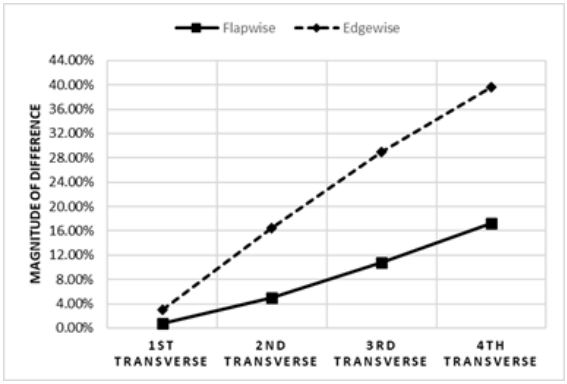

(a) Uniform Beam

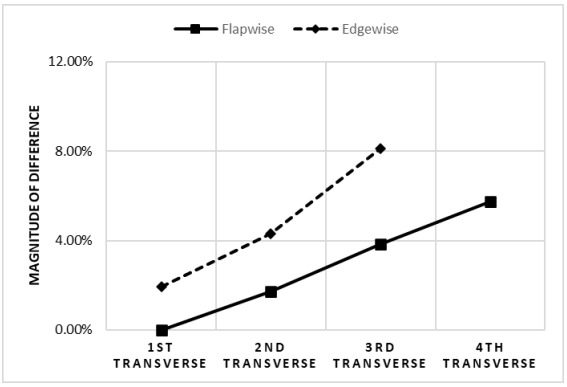

(b) Wind Turbine Blade

Figure 1 – Differences between FEM results for EB and TBT.

5 Application case: reference wind turbine blade

The blade analyzed in this paper is the DTU 10MW Reference Wind Turbine (RWT) blade, described in Bak et al. [3]. The authors provide the properties for 51 sections of that blade and the first eight natural frequencies, which are presented on Table 2, and were calculated using an aeroelastic code developed by the DTU called HAWC2.

In this work some assumptions were made to simplify the FEM implementation:

- The elastic axes of all sections were considered colinear;
- The mass center and the geometric center of each section were considered coincident;
- The torsion angles between the sections were not considered.

The FEM results for EB and TBT are compared to Bak et al. [3] results in Table 2. For most of the modes (six out of eight) the agreement is very good, with differences below 3% for EB and below 6% for TBT. However, high differences were observed for the 1st Torsion mode (14.98% for both models) and for the 3rd Edgewise mode (-9.50% for EB and -16.83% for TBT). It is believed that the high differences for these two modes are due to the assumptions considered. Further work is planned to assess the impact of removing these assumptions on the results.

Regarding the comparison between EB and TBT results, also presented in Table 2, it can be seen that, as for the case of the uniform beam, the frequencies obtained by TBT are lower than the ones obtained by EB (with exception of the torsion mode which has the same value). The magnitude of the difference between both methods also increases with mode order, being of about 8% for the 3rd Edgewise mode. This behavior is illustrated in Figure 1 (b).

Table 2 – Natural frequency results for wind turbine blade.

Description	Freq. Bak et al. (Hz)	Freq. FEM EB (Hz)	Difference EB	Freq. FEM TBT (Hz)	Difference TBT	Difference EB and TBT
1st Flapwise	0.61	0.61	0.00%	0.61	0.00%	0.00%
1st Edgewise	0.93	0.94	1.20%	0.92	-0.75%	-1.92%
2nd Flapwise	1.74	1.73	-0.34%	1.70	-2.47%	-2.14%
2nd Edgewise	2.76	2.83	2.62%	2.71	-1.81%	-4.31%
3rd Flapwise	3.57	3.58	0.25%	3.44	-3.59%	-3.84%
1st Torsion	5.69	6.54	14.94%	6.54	14.94%	0.00%
4th Flapwise	6.11	6.10	-0.23%	5.75	-5.95%	-5.73%
3rd Edgewise	6.66	6.03	-9.50%	5.54	-16.83%	-8.10%

6 Conclusions

Computational codes based on the Finite Element Method were implemented with Euler-Bernoulli and Timoshenko beam formulations to obtain natural frequencies of a uniform cantilever beam and a wind turbine blade. The implementation of the codes was validated comparing computational results obtained for the uniform beam with theoretical results. The application of the codes to the wind turbine blade provided reasonable results in comparison with the ones available in the literature. The discrepancies are believed to be due to the assumptions made, which will be a topic for further investigation.

Analyzing both model results, it was possible to assess the effects of the inclusion of the shear stress and rotatory inertia by the Timoshenko Beam Theory, which reduces the values of the natural frequencies for the transverse modes, both for the uniform beam and for the wind turbine blade.

For the case of the wind turbine blade, a maximum magnitude difference of about 8% was obtained between Euler-Bernoulli and Timoshenko models. This number can have some significance for all engineering calculations that depend on the natural frequencies as input parameters.

Authorship statement. The authors hereby confirm that they are the sole liable persons responsible for the authorship of this work, and that all material that has been herein included as part of the present paper is either the property (and authorship) of the authors, or has the permission of the owners to be included here.

References

[1] M. H. Hansen, "Aeroelastic Instability Problems for Wind Turbines". *Wind Energy*, vol. 10, pp. 551–577, Wiley Interscience, 2007.
[2] L. Wang, X. Liu, A. Koliosa, "State of the Art in the Aeroelasticity of Wind Turbine Blades: Aeroelastic Modelling". *Renewable and Sustainable Energy Reviews*, vol. 64, pp. 195-210, Elsevier, 2016.
[3] C. Bak et al, "Description of the DTU 10 MW Reference Wind Turbine". DTU Wind Energy Report-I-0092.
[4] R. D. Blevins, "Formulas for natural frequency and mode shape". Litton Educational Publishing, Inc., 1979.
[5] S. S. Rao, "Mechanical Vibrations". 5. ed. Pearson Education, Inc., 2011.
[6] D. J. Inman, "Engineering Vibrations". 4. ed. Pearson Education, Inc., 2013.
[7] R. R. Craig and A. J. Kurdila, "Fundamentals of Structural Dynamics". 2. ed. John Wiley & Sons Inc., 2006.
[8] T. C. Huang, "The Effect of Rotatory Inertia and of Shear Deformation on the Frequency and Normal Mode Equations of Uniform Beams With Simple End Conditions". *Journal of Applied Mechanics*, vol. 28, n. 4, pp. 579-584, 1961.
[9] R. D. Cook, D. S. Malkus, M. E. Plesha and R. J. Witt, "Concepts and Applications of Finite Element Analysis". 4. ed. John Wiley & Sons, Inc., 2002.
[10] J. S. Przemieniecki, "Theory of Matrix Structural Analysis". 1. ed. McGraw-Hill, Inc., 1968.
[11] W. C. Young and R.G. Budynas, "Roark's Formulas for Stress and Strain". 7. ed. McGraw-Hill, Inc., 2002.